# Ocean–Atmosphere Interaction and the Tropical Climatology. Part II: Why the Pacific Cold Tongue Is in the East

HENK A. DIJKSTRA

*Institute for Marine and Atmospheric Research, University of Utrecht, Utrecht, The Netherlands*

J. DAVID NEELIN

*Department of Atmospheric Sciences, University of California at Los Angeles, Los Angeles, California*

(Manuscript received 17 August 1994, in final form 1 December 1994)

ABSTRACT

The influence of coupled processes on the climatology of the tropical Pacific is studied in a model for the interaction of equatorial SST, the associated component of the Walker circulation, and upper-ocean dynamics. In this part, the authors show how different physical mechanisms affect the spatial pattern of the Pacific warm pool and cold tongue in this coupled climatology. When model parameters give a suitable balance between effects of upwelling and thermocline depth on sea surface temperature and for suitable atmospheric parameters, a good prototype for the observed cold-tongue configuration is produced. This is largely determined by coupled ocean–atmosphere processes within the basin. Presence of an easterly wind stress component produced by factors external to the Pacific basin can be important in setting up a cooling tendency, but this is magnified and modified by a chain of nonlinear feedbacks between trade winds and ocean dynamics affecting the SST gradient within the basin. These feedbacks determine a preferred spatial pattern that does not strongly depend on the form of the external wind stress and that tends to place the cold tongue in the east-central basin. Although robust to external influences, this pattern is sensitive to the balance of coupled processes. Parameter changes can produce warm-pool–cold-tongue patterns significantly different from observed but resembling some noted in coupled GCMs.

## 1. Introduction

Coupled ocean–atmosphere processes substantially determine the spatial structure of the tropical Pacific climatology. We have referred to this statement in Neelin and Dijkstra (1995; ND hereafter) as the "climatological version of the Bjerknes hypothesis." Our focus is on the equatorial Pacific sea surface temperature (SST) and its interaction with the Walker circulation. While part of the Pacific trade winds is forced by factors outside the basin, the gradients in SST generate a substantial part of the annual mean low-level winds over the basin, and these in turn affect the SST pattern. This conjecture—that the internal coupled feedbacks within the Pacific significantly enhance and modify SST gradients imposed by external factors—suggests that the Pacific cold-tongue–warm-pool configuration should be regarded as a coupled phenomenon on a par with ENSO, to which the Bjerknes' (1969) hypothesis applied.

*Corresponding author address:* Dr. J. David Neelin, Department of Atmospheric Sciences, University of California at Los Angeles, Los Angeles, CA 90024-1565.
E-mail: neelin@atmos.ucla.edu

In this series of papers, we set up and analyze a simple prototype for these interactions using the model of Neelin and Jin (1993; collectively referred to as JN with Jin and Neelin 1993a,b) in combination with continuation methods (Dijkstra and Neelin 1995, hereafter DN). In Part I (ND) we presented the basic setup and showed how these coupled feedbacks produce dramatic differences between flux-corrected and non-flux-corrected (fully coupled) versions of the model. By flux-correction, we mean any of several techniques that are used to artificially dictate a climatological state (resembling observed) to avoid having to simulate this state within the coupled system. Neelin and Dijkstra (1995) showed that the same feedbacks that contribute to the maintenance of the cold tongue in the fully coupled system can create spurious multiple stationary states in the flux-corrected system; they also discussed the relation between the two systems. In the fully coupled system, only a single-solution branch generally exists for the coupled climatology. This branch, which we determined in ND for only a particular choice of parameters, is the starting point of this paper.

In section 2, we outline our approach, attempting to justify in more general terms the approach applied in this simple prototype system. We find it useful to distinguish between the contribution to the wind stress

over the basin that is due to external factors, $\tau_{ext}$, and the contribution due to coupled feedbacks within the basin; we attempt to generalize this before specializing to the simpler system. Section 3 then sketches the particular setup of the model used here.

The evolution of the coupled climatology as a function of strength of coupled feedbacks is presented in section 4, along with an examination of parameter dependence. This is used to argue that despite its simplifications the model is capable of simulating a reasonable cold tongue and to discuss processes that affect the spatial configuration. Section 5 pursues the relative role of $\tau_{ext}$ versus internal feedbacks in determining the cold tongue and includes experiments that isolate various mechanisms by which $\tau_{ext}$ contributes. In section 6, we consider the role of spatial structure in $\tau_{ext}$ and provide an example of how coupled processes can overcome $\tau_{ext}$ to produce the cold-tongue structure preferred by internal coupled dynamics.

In ND we noted that the sensitivity of the tropical Pacific climatology in coupled GCMs (e.g., Endoh et al. 1991; Gent and Tribbia 1993; Latif et al. 1993; Latif et al. 1994; Lau et al. 1992; Mechoso et al. 1993, 1994; Meehl 1990; Nagai et al. 1992; Philander et al. 1992; Robertson et al. 1995; Sperber et al. 1987), especially low-resolution models or earlier versions of high-resolution models, provides circumstantial evidence for the role of coupled feedbacks (Neelin et al. 1992). Climate drift—the departure of the model equilibrium climatology from observed—is worse for the coupled models than for the uncoupled components. Small errors in the uncoupled ocean or atmosphere model (e.g., an error in the radiative equilibrium temperature) are exacerbated due to coupling and influence the resulting climatology. These amplified errors may lead to an incorrect position or form of the cold tongue, examples of which were found in many early GCMs (e.g., Sperber et al. 1987; Meehl 1990). Section 7 aims to make the connection between the conclusions regarding the coupled climatology from the prototype system, on the one hand, and problems faced by the coupled GCMs, on the other. Scenarios for the roles of coupled feedbacks in climate drift are outlined. Conclusions are in section 8.

## 2. Approach

Even if there were no longitudinal gradients of SST, there would still be a Hadley circulation and a Walker circulation driven, respectively, by zonally symmetric latitudinal gradients and zonally asymmetric land–sea contrast, topography, etc. (Stone and Chervin 1984). In tackling the role of coupling between ocean dynamics, SST, and Walker circulation, it is helpful if we can separate, at least approximately, contributions to the atmospheric circulation over the basin that (i) are affected by coupled feedbacks on SST within the basin or (ii) do not depend on these and can be regarded as external to the coupled processes within the basin. In a simple model, it is straightforward to specify such a distinction, particularly since we focus here only on feedbacks involving wind stress. To justify and provide context for this, we first attempt to outline procedures by which this distinction could be made in more complex models.

In the simple model, the wind stress field passed to the ocean model has the form outlined in ND as a prototype for the coupled system without flux correction:

$$\tau = \tau_{ext} + \mu A(T - T_0), \qquad (1)$$

where $\tau_{ext}$ represents the wind stress contribution from factors external to the feedbacks within the basin, $T$ is SST, $T_0$ is the surface temperature in absence of ocean dynamics, and $A$ is the operator from the atmospheric model that yields wind stress response to a given temperature pattern. In the simple model, the case of annual average conditions is treated, so $T_0$ is assumed to be determined by surface heat flux equilibrium and is further idealized as independent of longitude. The coupling parameter $\mu$ is a scalar parameter that can be used to go conveniently between the uncoupled problem—where no feedbacks occur between wind and ocean dynamics within the basin—and the coupled problem, in order to understand the processes involved.

To generalize the separation embodied in (1), consider GCM experiments in which an atmospheric GCM has continental or specified-SST boundary conditions outside the basin of interest. By running an ensemble of GCM integrations, one wishes to determine $\tau_{ext}$. The question is what boundary conditions should be specified within the basin and how to handle $T_0$ and its GCM equivalent. If the distinction is posed as "what is the part of the wind stress not associated with feedbacks with ocean dynamics or ocean mixed layer memory?," then specifying a zero heat capacity, swamp boundary condition within the ocean basin is appropriate. The resulting wind stress over the basin can be regarded as $\tau_{ext}$ and the surface temperature over the basin as $T_0$. To avoid potential problems with either effects of high-frequency motions or the seasonal cycle, it may be better in practice to pose the distinction as "what is the part of the wind stress not associated with feedbacks with ocean dynamics?" and to regard the ocean mixed-layer memory as part of the "external" problem, that is, to include a finite mixed layer heat capacity in the lower-boundary conditions specified over the basin. The resulting winds and temperature are still regarded as $\tau_{ext}$ and $T_0$ but for this slightly different problem. For the annual average case, one might hope that the results would have only a weak dependence on mixed-layer heat capacity, so these two approaches would give similar results. Finally, there can be interesting feedbacks involving effects of cloud-

iness, wind speed, etc., in addition to ocean dynamics interacting with longitudinal variations of SST. If the distinction is posed as "what is the part of the wind stress not associated with feedbacks with longitudinal gradients of SST," then an appropriate surface boundary condition would be the equivalent of placing longitudinally conducting rods of a given heat capacity (zero or for a mixed layer) across the basin. SST gradients would be zero across the basin, but the latitudinally varying $T_0$ would be appropriate to the heat flux balance averaged across the basin. In the simple model, the approach mimics the results of either of the first two of these setups, and the simplifications do not strongly distinguish these from the third.

Such GCM experiments have not been performed; the closest experiments in the literature are those of Chervin and Druyan (1984) and Stone and Chervin (1984) conducted in a coarse (8° latitude) resolution GCM in perpetual January. The experiments we advocate are in the spirit of theirs—which sought to separate the effect upon the Walker circulation of SST gradients, continents, etc.—but the boundary conditions differ. Their closest cases are (i) warm western Pacific SST replacing SSTs at all longitudes in a tropical band and (ii) SSTs replaced by their zonal average. It is difficult to say how well either case approximates the situation we are interested in—namely the circulation in absence of tropical ocean dynamics—because latitudinal ocean transports cool observed zonal mean tropical SST relative to neighboring continental regions. In both cases, however, there is a very substantial reduction (in the first case a total collapse) of the low-level trades over the Pacific.

We are thus obliged to specify $\tau_{ext}$ a priori. The choices of $\tau_{ext}$ are intended to be simple and plausible but are also aimed at demonstrating that the spatial form is, in some cases, unimportant to the coupled solution. The greatest simplification is that we include only zonal stress, symmetric about the equator, consistent with other simplifications in the model, discussed below. We use as a standard a zonally constant zonal stress denoted $\tau_z$. This is partly chosen on physical grounds since regardless of the details of the longitudinal SST gradients within the basin there will be a modest but significant easterly stress component due to the global Hadley circulation. Further, because of the simplicity of the specified spatial pattern, it allows the patterns developed internally by coupling to be more clearly seen. We also test cases with differing spatial patterns for $\tau_{ext}$, in particular, additional easterlies, $\tau_I$, near the "Indonesian" region, such as might be created by a heat source over warm water or a continental region just to the west of the basin:

$$\tau_{ext}(x) = \tau_z + \tau_I(x) . \qquad (2)$$

This is both physically relevant for the Pacific (see also Yamagata and Masumoto 1989) and tends to create a cold tongue in the west for the uncoupled case, thus providing a nice example of the effects of coupled feedbacks.

If the simple ocean model is driven by $\tau_{ext}$, it produces an SST pattern that we denote $T_{ext}$. An important aspect of the coupled versus uncoupled problem is that, if $\tau_{ext} \neq 0$ then $T_{ext} \neq T_0$, so that $T_{ext}$ is *not* a solution when coupling is nonzero. As a consequence (see ND) no bifurcation is needed to initiate coupled feedbacks that deepen the cold tongue (hence the absence of multiple stationary states in the coupled climatology solution). In the coupled GCM case, there is no simple parameter corresponding to $\mu$ leading between the fully coupled solution and the uncoupled $T_{ext}$ solution, but these two can still be compared. To define $T_{ext}$, drive the ocean GCM with $\tau_{ext}$ and an appropriate surface flux condition (which could involve coupling to the atmospheric GCM through heat flux only or a simple heat flux condition using information from $T_0$ and the associated surface fluxes). Contrasting $T_{ext}$ and associated ocean dynamics to the solution from the full coupled GCM would show the impact of coupled feedbacks in a manner similar to the simple model case.

## 3. Model setup

The same coupled model as in ND is used, aside from parameter changes, except here the fully coupled case is explored. While time-dependent versions of this model are classed as coupled models of intermediate complexity when applied to the ENSO problem, the steady version presented here can be considered as a simple coupled model with respect to the coupled climatology problem. Ocean dynamics affects SST most strongly along the equatorial strip, and two of the most important contributions are the east–west thermocline tilt and equatorial upwelling, both of which are most strongly affected by zonal wind. For this prototype problem, we can thus employ the equatorial band approximation in SST (Neelin 1991) to study these interactions. We further idealize to a situation symmetric in latitude about the equator. In the observed cold tongue, of course, there is significant north–south asymmetry associated with the ITCZ north of the equator (e.g., Mitchell and Wallace 1992). Xie and Philander (1994), Xie (1994), and Philander et al. (1994, personal communication) present evidence that this latitudinal asymmetry is itself an interesting coupled phenomenon, in essence complementary to the problem addressed here. At the current level of approximation, it appears these aspects can initially be studied separately, since north–south asymmetries appear not to be crucial to the main symmetric interactions. We know from uncoupled climatologies forced by annual average equatorial zonal wind stress that reasonable equatorial Pacific SST can be achieved in ocean models (Hao et al. 1993; Jin and Neelin 1993a;

TABLE 1. Main model parameters and best values (nondimensional).

| | | |
|---|---|---|
| $\mu$ | Coupling parameter | 0.5 |
| $\delta_s$ | Surface-layer parameter | 0.5 |
| $\epsilon_a$ | Atmospheric inverse damping length | 2.5 |

DN) that have symmetric latitudinal structures. This assumption most likely limits applicability of the current model to the Pacific since Indian and Atlantic Oceans have pronounced latitudinal asymmetries associated with land masses, although the approach of section 2 holds more generally.

The wind stress fed into the ocean model is given by (1), where $\tau_{ext}$ is a given function of $x$ and where the wind stress feedbacks are produced by a simple Gill atmospheric model, with specified latitudinal structures of the SST departures from surface heat-flux equilibrium. The essential equations for the atmosphere, shallow-water ocean dynamics, surface-layer currents, and equatorial band SST equation are given in the appendix. Table 1 summarizes the main parameters used in this study.

For ease of reference, we define the SST and thermocline depth $h$ for the uncoupled case—the ocean response to $\tau_{ext}$ forcing—as $T_{ext}$ and $h_{ext}$, respectively. We use the terms "thermocline feedback" to denote interactions involving changes in $h$ and "surface-layer feedback" to denote interactions involving Ekman currents associated with the embedded surface layer [second term in (A3)]. Zonal advection of SST, normally included in the latter, produces feedbacks similar to upwelling in terms of spatial relations between fields but plays a secondary role and therefore has been omitted for clarity here.

For hypothesis testing purposes, we employ modifications to the model to eliminate or simplify certain interactions. These modifications are described in the relevant sections with the results of the experiments.

## 4. Coupled feedbacks and the cold tongue

In this section, we investigate the variation of the climatology with respect to the internal coupled feedbacks while keeping a constant external windstress $\tau_z$. Then the structure of the steady states is controlled by the parameters $\epsilon_a$, $\delta_s$, and $\mu$. For $\tau_z = -0.2$ (which corresponds to a value of the external windstress of about 0.01 Pa), the externally forced thermocline and SST, denoted $h_{ext}$ and $T_{ext}$, are shown in Fig. 1; upwelling is constant across the basin. The temperature decreases monotonically from west to east and the thermocline profile is linear. The cold tongue for this case is weak and, rather than flatten in the east-central basin, the zonal temperature gradient increases all the way to the eastern coast.

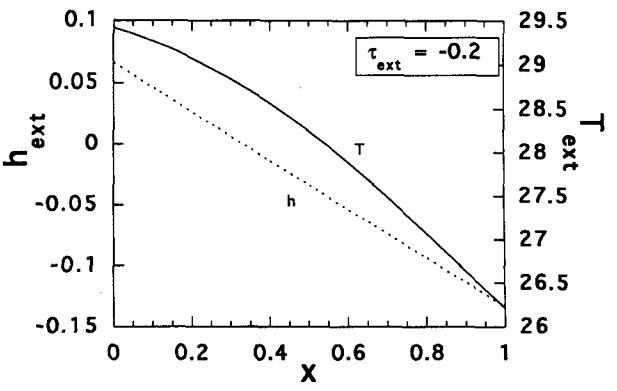


FIG. 1. Equatorial SST and thermocline depth (departure from rest state) for the uncoupled ocean solution driven by externally specified wind stress $\tau_{ext}$. Here zonally constant easterlies are used: $\tau_{ext} = \tau_z = -0.2$ (nondimensional) $\approx -0.01$ Pa (dimensional).

Figure 2 presents bifurcation diagrams, showing how coupling influences the structure of the steady states, for three values of $\delta_s$. The case of $\epsilon_a = 1.25$ (i.e., a relatively long atmospheric damping scale, comparable to the basin length) is chosen here for illustration of the behavior. In each bifurcation curve there is a unique solution for the climatology at each $\mu$, but the feedback between additional trade winds, upwelling, and thermocline slope within the basin rapidly modifies the solution as coupling is increased. Spatial structures of the solutions for standard $\delta_s$ may be seen in Fig. 3 for several coupling values. At low coupling (Figs. 3a–b), the additional wind stress due to coupling is approximately the atmospheric response to the original cooling, $T_0 - T_{ext}$, which increases easterlies over most of the

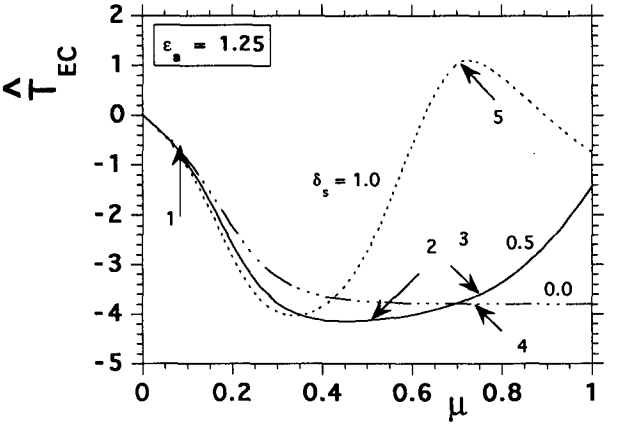


FIG. 2. Coupled climatology solution as a function of the coupling parameter $\mu$. SST at a point $x = 0.7$ in the east-central Pacific, $T_{EC}$, is shown as departure from the uncoupled value (driven by $\tau_{ext}$ alone): $\hat{T}_{EC} = T_{EC} - T_{ext|EC}$. Curves are for strong ($\delta_s = 1.0$; dotted lines) moderate ($\delta_s = 0.5$; solid line) and zero (dash-dotted line) values of the surface-layer feedback. Labels indicate points where longitudinal plots are presented in subsequent figures.

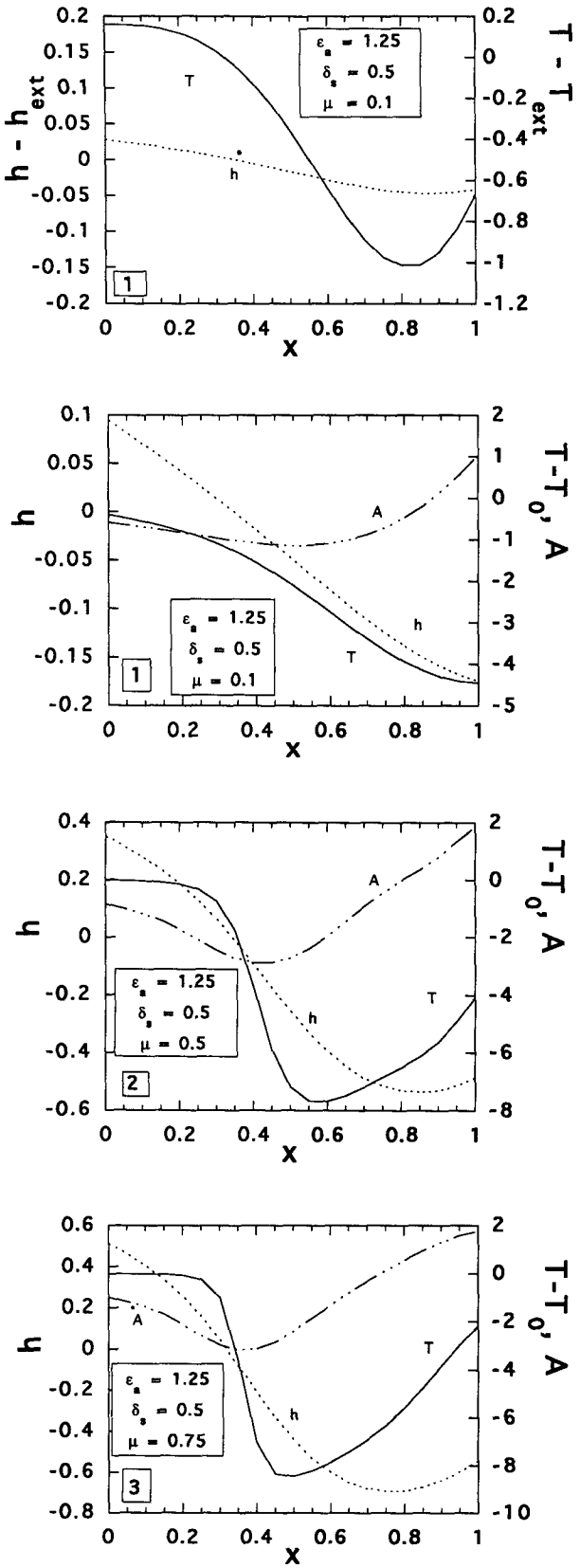


basin, except in the eastern most part. The preference for easterlies is due to the east–west asymmetry introduced by $\beta$ (the latitudinal gradient of the Coriolis parameter) in the atmospheric model, which gives easterlies over the west of a large-scale cool SST region, with westerlies near the eastern edge and to the east.

At reasonable values of the coupling (Fig. 3c), the increased wind stress produces both greater upwelling over the central part of the basin, which tends to shift the cold tongue westward, and greater thermocline slope, which tends to keep the cold tongue eastward. The compromise between these processes creates a broad minimum in the east-central basin. The wind stress pattern is shifted slightly westward relative to the low coupling case and is modified to accord with the SST pattern, but the winds remain of broad spatial scale and easterly except in the easternmost part of the basin. A westerly contribution in the east tends to cancel $\tau_z$, resulting in a flat thermocline in this region and reduced upwelling, which causes a slight warming at the east edge of the cold tongue. At stronger coupling (Fig. 3d), all these processes are accentuated, resulting in overly strong gradients between warm pool and cold tongue (associated with the strong thermocline gradient and the model's $T_{sub}$ parameterization) and considerable reduction in the cold tongue near the east coast.

The balance between thermocline feedback and surface-layer feedback strongly affects the preferred spatial form of the cold tongue. Figure 4 shows cases where the surface-layer feedback is alternately shut off or increased (strong coupling is used to highlight the differences). For the solution in Fig. 4a (point 4, $\delta_s = 0$), only the thermocline feedback is active. Since there is only externally induced upwelling, SST departures from $T_0$ are governed by the temperature of the upwelled water. The thermocline is deep in the west and very shallow in the east, giving temperatures nearly equal to the surface equilibrium temperature in the west. The cold tongue has constant temperature in the east due to saturation at minimum subsurface temperature. This SST configuration is consistent with increased easterlies over almost the entire basin. Figure 4b shows the case of strong surface-layer feedbacks (point 5, $\delta_s = 1.0$). Because the effect of wind modifications on upwelling is stronger, the cold tongue shifts west toward the region of maximum easterlies, which in turn shifts farther west. The deep thermocline in the western Pacific limits this process. On the eastern

FIG. 3. Longitudinal dependence along the equator of coupled solutions for labeled points in Fig. 1. Case of moderate surface-layer feedbacks (standard $\delta_s = 0.5$) with $\epsilon_a = 1.25$. (a) $\mu = 0.1$. Thermocline depth and SST are shown as departures from the uncoupled solution, $h - h_{ext}$ and $T - T_{ext}$. (b) $\mu = 0.1$, showing total solutions for thermocline depth $h$ (as departure from rest state) and SST relative to the surface-flux equilibrium, $T - T_0$. Atmospheric wind stress response is shown for the component associated with coupled feedbacks, $A$ (nondimensional). (c) $\mu = 0.5$, as in (b). (d) $\mu = 0.75$, as in (b).

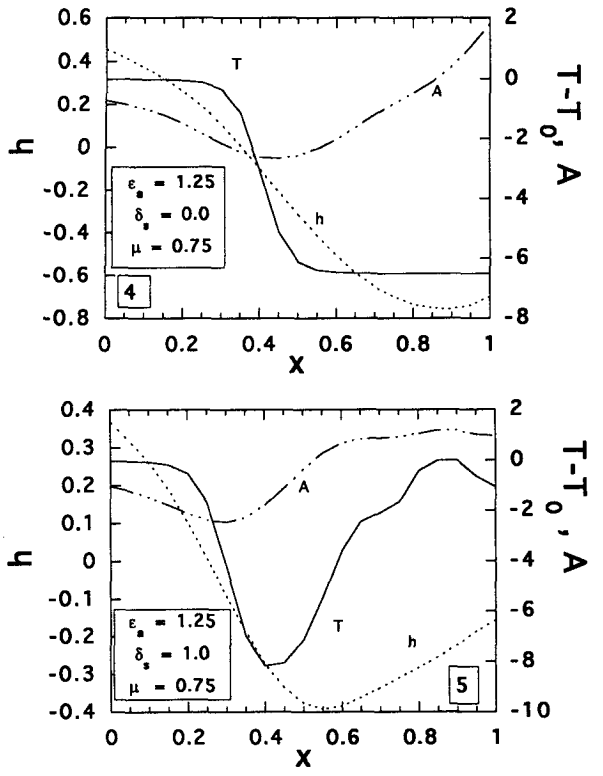


FIG. 4. As in Fig. 3b but for cases of zero and strong surface-layer feedbacks. (a) $\delta_s = 0.0$, $\mu = 0.75$. (b) $\delta_s = 1.0$, $\mu = 0.75$.

side of the basin, westerly perturbations almost cancel $\tau_z$, giving greatly reduced upwelling and consequent warming. A narrow cold tongue in midbasin results. Implications of this sensitivity of the cold-tongue pattern to the relative balance of upwelling versus thermocline feedbacks will be discussed further below.

Results so far have used the case of relatively small $\epsilon_a$ so that it is clear that the decay scale in the atmosphere is not the primary length scale. We now consider the effects of more realistic $\epsilon_a$; bifurcation diagrams for the standard value of $\epsilon_a$ and an intermediate value are presented in Fig. 5, with spatial patterns in Fig. 6. An increase of $\epsilon_a$ leads to a more localized response of the wind field. The cold-tongue configuration is qualitatively similar over a broad range of $\epsilon_a$. The tendency for the cold tongue to deepen more rapidly with coupling for the smaller $\epsilon_a$ used in Fig. 3 is largely an artifact of the nondimensionalization, which was carried out for standard $\epsilon_a$ and scales a factor proportional to $\epsilon_a$ into $\mu$ [compare (A1) with Neelin and Jin Eq. (2.9)]. When rescaled, the curves in Figs. 3 and 5 are rather similar, although effects from the spatial extent of the wind response on the strength of the thermocline feedback may be noted.

The most significant effect of $\epsilon_a$ is on the spatial pattern. Contrary to what might be expected, decreases in the atmospheric spatial scale (larger $\epsilon_a$) are not associated with narrower spatial scale for the cold tongue in this range (compare Fig. 6b with Fig. 3c). Rather, the main effect is to move the cold-tongue minimum eastward. This is because larger $\epsilon_a$ tends to deemphasize the easterly response to the west of a cold region relative to the response within the region. This reduces upwelling to the west and shifts the region of shallowest thermocline, with consequent feedbacks on SST.

At $\epsilon_a = 2.5$ (point 1, Figs. 6a–b), the cold tongue is situated at a reasonable position ($x = 0.8$), and the extent of the SST minimum and the slight increase in SST at the east coast are quite satisfactory. In fact, the climatology looks very much like that of a flux-corrected climatology forced with an approximation to observed wind stress (compare Fig. 1 in DN). If the coupling is increased for $\epsilon_a = 2.5$, again perturbation downwelling causes a rise in temperature at the east coast (point 2, Fig. 6c, $\mu = 1$), and also the cold tongue becomes broader and the minimum is shifted back to the west. Slight changes in $\epsilon_a$ (point 3, Fig. 6d) make only a modest difference but tend to shift the cold tongue minimum. Hence, there is an optimum simulation for the region in parameter space near $\epsilon_a = 2.5$, $\delta_s = 0.5$, and $\mu = 0.5$ (Figs. 6a–b). The main point of the results in the Figs. 6a–b is therefore that a reasonable climatology (cold-tongue position, shape, and amplitude) can be generated through coupled feedbacks and a relatively small constant external wind stress ($\tau_z$) in this simple model. The shape and size of the contribution by coupled feedbacks in Fig. 6a relative to the externally driven contribution in Fig. 1 neatly illustrates the importance of coupling.

## 5. Importance of external wind stress via upwelling versus thermocline slope

Having established the sensitivity to major parameters and the range for which a good prototype cold

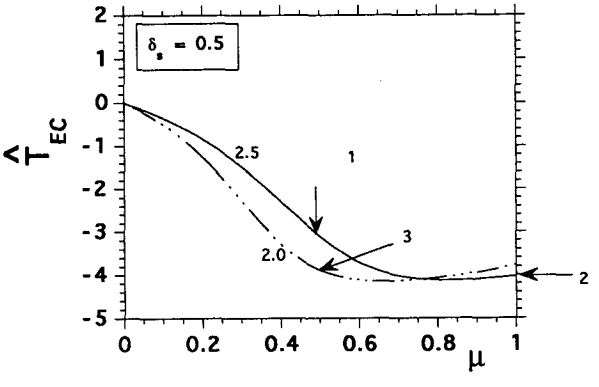


FIG. 5. As in Fig. 2 but for $\delta_s = 0.5$ and two values of the atmospheric damping $\epsilon_a$. Labels indicate points for which longitudinal plots are presented. Point 1 is the standard case corresponding to the "best" parameter values given in Table 1.

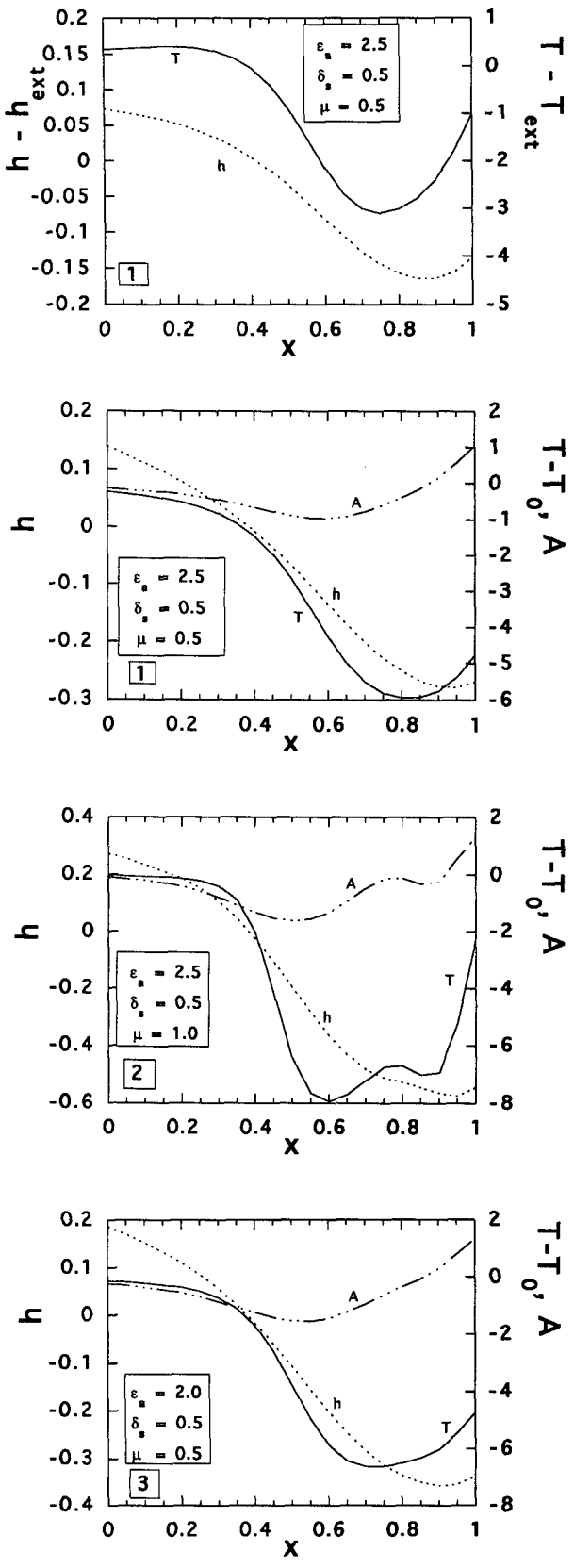


tongue is generated by internal feedbacks, we consider in this and the next section the influence of the magnitude and the spatial structure of the external forcing. For the case $\tau_{ext} = \tau_z$, with no longitudinal structure, the results of the previous section showed that coupled feedbacks modify the externally induced zonal SST gradient ($T_{ext}$ in Fig. 1). The amplitude of $\tau_z$ is expected to be unimportant for the spatial structure, except that it controls the magnitude of externally induced upwelling and therefore the overall strength of the feedbacks setting up the cold tongue. This is indeed seen in Figs. 7a–b, where the equilibrium structures (for $\epsilon_a = 2.5$, $\mu = 0.5$, $\delta_s = 0.5$) are shown for different $\tau_z$. The position of the cold tongue hardly changes; $\tau_z$ merely controls the amplitude of the temperature deviation from the equilibrium value, not its spatial structure.

A constant $\tau_z$ induces both external upwelling, say $w_{ext} = -\delta_F \tau_z$, and a thermocline slope through $h_{ext}(x) = (x - 1/3)\tau_z$, as in Fig. 1. The latter introduces an east–west asymmetry within the basin. To investigate whether this slope in the thermocline is important to obtain a correct east–west structure, we decouple $w_{ext}$ and $h_{ext}(x)$. One way to do this is to introduce an entrainment velocity $w_0$, independent of $\tau_z$, associated with mixing at the base of the mixed layer that would occur even if large-scale winds were zero. Hence, the vertical advection plus entrainment term in the SST equation becomes

$$[w_0 + \mathscr{H}(w_z + w_c)(w_z + w_c)](T - T_{sub}), \quad (3)$$

where we define $w_z$ and $w_c$ to be the components of the Ekman upwelling $w_1$ induced by the constant external windstress $\tau_z$ and by wind stress due to coupled feedbacks $\mu A$.

As an extreme case, we take the externally induced climate to consist of a flat thermocline and constant upwelling; this case is of fundamental interest. When coupling breaks the zonal symmetry (within the basin) into a correct east–west structure, the processes involved are those essential to the question of why the cold tongue is in the east. For this case, we take the limit $\tau_z \to 0$ and hence $h_{ext} = 0$, while keeping $w_0 > 0$. For $\tau_z \to 0$, by definition $w_z$ vanishes and at $\mu = 0$ the temperature will be constant over the basin (and slightly lower than the equilibrium temperature) due to $w_0$. Note that zonal symmetry in the strict sense is already broken by the difference between SST and the equilibrium temperature $T_0$ of the surrounding land. In the model, this problem can be efficiently handled

FIG. 6. As in Fig. 3 but for labeled points in Fig. 5. (a) Standard case, $\epsilon_a = 2.5$, $\delta_s = 0.5$, $\mu = 0.5$; departures from uncoupled as in Fig. 3a. (b) Standard case, $\epsilon_a = 2.5$, $\delta_s = 0.5$, $\mu = 0.5$, total fields, as in Fig. 3b. (c) As in (b) but $\mu = 1.0$. (d) As in (b) but $\epsilon_a = 2.0$.

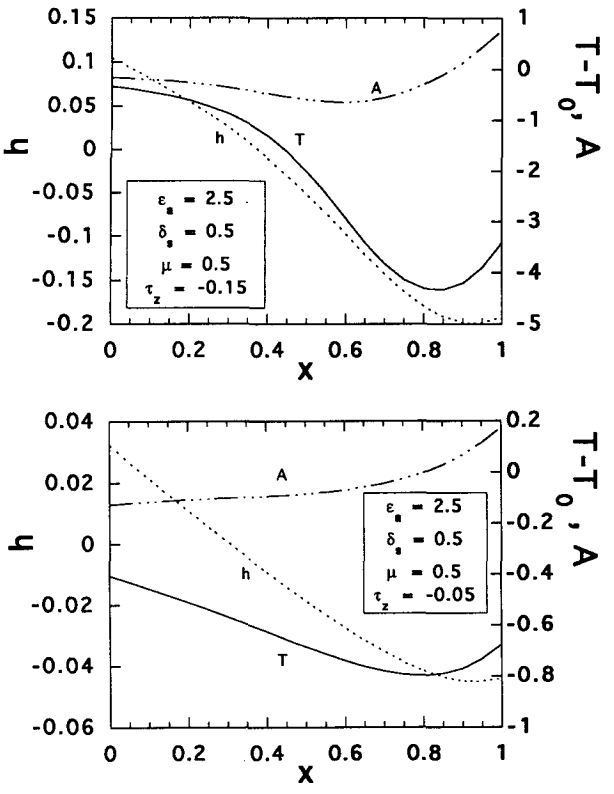


FIG. 7. As in Fig. 6b but for two values of the zonally constant external wind stress, $\tau_{ext} = \tau_z$ (nondimensional): (a) $\tau_z = -0.15$, (b) $\tau_z = -0.05$.

by the continuation techniques by introducing an artificial parameter $\alpha_S$, which controls $h_{ext}$ as a function of $\tau_{ext}$ in (1d). Specifically

$$h_{ext}(x) = \alpha_S \left\{ \int_0^1 s^{1/2} \tau_{ext}(s)\, ds - \int_x^1 \tau_{ext}(s)\, ds \right\}. \quad (4)$$

If $\alpha_S = 1.0$, there is externally induced zonal asymmetry (the case we have considered up until now) and $w_0 = 0$, whereas for $\alpha_S = 0.0$, $h_{ext}$ vanishes and a constant $\tau_z$ is then equivalent to a constant entrainment velocity $w_0 = -\delta_F \tau_z$ at the base of the mixed layer. In this way, we can continuously deform the steady states from the cases already considered to nontrivial solutions in the case of constant upwelling. A standard value of $\tau_z = -0.2$ corresponds to $w_0 = 0.8$, which corresponds to an upwelling velocity of 0.5 m day$^{-1}$.

For parameter values at the optimum situation in section 3 ($\epsilon_a = 2.5$, $\delta_s = 0.5$), the bifurcation pictures for four combinations of $\delta_s$ and $w_0$ are presented in Fig. 8, with corresponding spatial patterns in Fig. 9. For $\delta_s = 0$, the spatial structure of the climatology at $w_0 = 0.4$ and $\mu = 1$ still looks reasonable (point 1, Fig. 9a). As the magnitude of $w_0$ increases, the eastern part of the basin becomes colder (point 2, Fig. 9b), and the cold tongue tends to shift farther eastward. An increase of the surface-layer activity (by increasing $\delta_s$) again causes downwelling in the east through the westerly winds. This shifts the cold tongue to the west and increases the temperature at the eastern boundary (point 3, Fig. 9c). For larger $w_0$, the spatial pattern remains the same and only the amplitude increases (point 4, Fig. 9d). If $\mu$ is decreased to $\mu = 0.5$ (our optimum case for $\alpha_S = 1.0$), the amplitude becomes far too small, even for $w_0 = 0.8$. Hence, a larger value of $\mu$ is required to get the same amplitude compared to the case where a thermocline departure $h_{ext}$ is induced by the external wind stress.

When the magnitude of the specified entrainment velocity is further decreased, significant changes occur in the bifurcation pictures (Fig. 10a) and spatial patterns (Figs. 10b–c). At $\delta_s = 0.0$, the thermocline feedback can maintain a cold tongue with broad structure, a minimum SST in the eastern basin, and a curvature of the SST qualitatively similar to the optimum case in the eastern basin but of very small amplitude (Fig. 10b). However, at $\delta_s = 0.5$, the upwelling feedback dominates because the small upwelling yields small thermocline feedback. Correspondingly, the cold tongue shifts westward and ends up with minimum SST at the west coast (point 2, Fig. 10c). As in Figs. 4a–b, this illustrates the importance of the relative balance of processes in determining the preferred shape of the cold tongue. The difference here is that the balance between surface-layer feedback and thermocline feedback is determined by the small entrainment-upwelling that prevails in the uncoupled state.

Thus the most important role of $\tau_{ext}$ is in providing an external upwelling (that can be equivalently provided by an entrainment velocity). The shape of the cold tongue at reasonable coupling does not depend strongly on this—provided it is not too small—al-

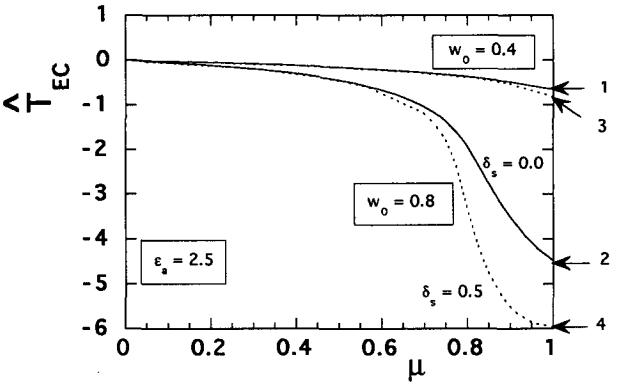


FIG. 8. As in Fig. 2 but for four combinations of $\delta_s$ and of the specified entrainment velocity $w_0$ in a modified version of the model. Upper curves $w_0 = 0.4$, lower curves $w_0 = 0.8$, solid lines $\delta_s = 0$, dashed lines $\delta_s = 0.5$ (standard). Other parameters standard. Labels indicate points for which longitudinal plots are presented.

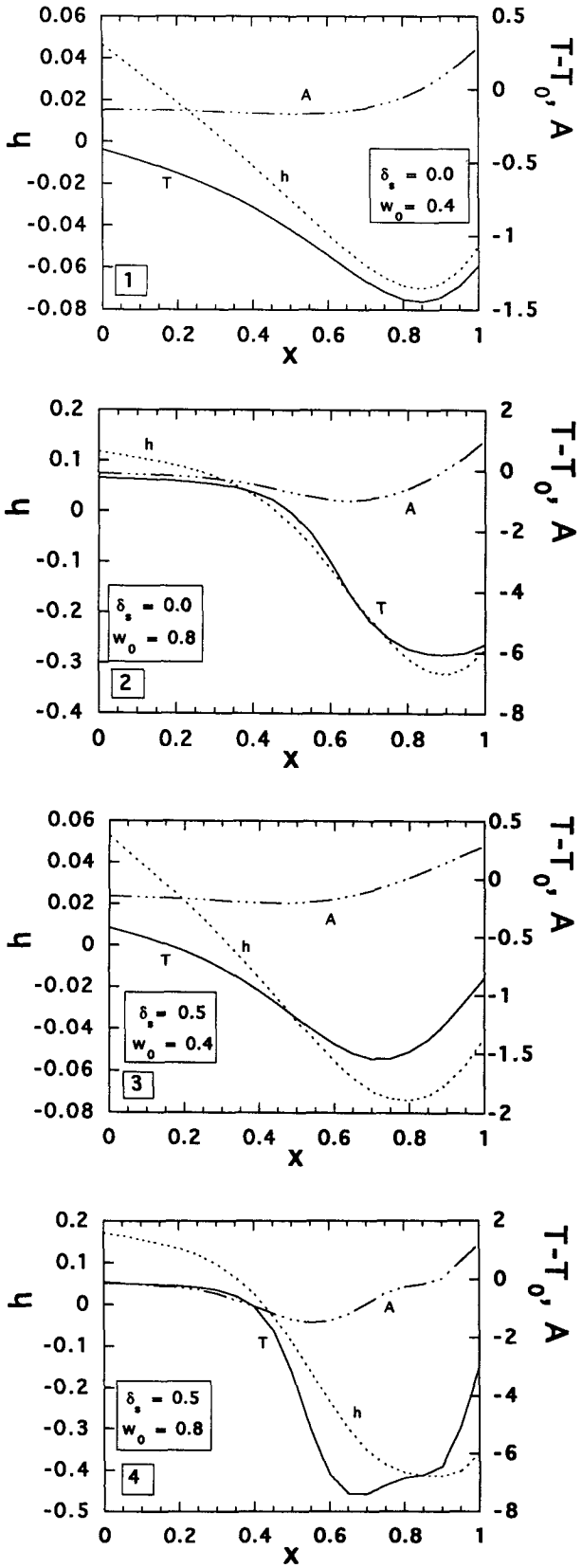


FIG. 9. As in Fig. 6b but for labeled points in Fig. 8, for the modified model. (a) Point 1; $\delta_s = 0$, $w_0 = 0.4$. (b) Point 2; $\delta_s = 0$, $w_0 = 0.8$. (c) Point 3; $\delta_s = 0.5$ (standard), $w_0 = 0.4$. (d) Point 4; $\delta_s = 0.5$, $w_0 = 0.8$.

though the amplitude of the cold tongue at reasonable coupling values does depend on it. Dimensionally, the minimum external upwelling required to meet this "not too small" condition is on the order of 0.1–0.2 m day$^{-1}$.

## 6. Longitudinal variation of $\tau_{ext}$ versus coupled feedbacks

Up to now, we have considered a spatially constant external wind stress. In section 3, coupled processes were able to modify the externally induced SST gradient to give an eastern cold tongue with characteristic structure. As outlined in section 2, the external wind stress may have zonal structure in addition to the zonally symmetric easterly component $\tau_z$. How are SST patterns associated with $\tau_{ext}$ structure modified through coupled processes, and what is the relative importance of thermocline slope and the upwelling?

To illustrate these effects, we consider the simple case of an additional external wind stress $\tau_I(x)$, which is only nonzero over an interval $[0, a]$ within the basin. This mimics the effect of heating over Indonesia or the Asian continent causing easterlies over the western part of the basin. We present the case

$$\tau_I(x) = 1.2(a - x)\mathscr{H}(a - x) \qquad (5)$$

with $a = 1/3$. Total wind stress, given by (2), includes $\tau_z$.

For $\tau_z = -0.1$ and $w_0 = 0$, the externally induced temperature field is plotted in Fig. 11a; the easterly $\tau_I$ causes a cold-tongue structure in the western part of the basin. The structure of the temperature in the east is similar to that caused by $\tau_z$ alone, with a thermocline sloping up to the east. At $\mu = 0.5$ (Fig. 11b), coupled processes have generated a cold tongue in the east similar to that found in absence of $\tau_I$. In the west, the structure is still affected by $\tau_I$ but less than in the uncoupled case. As $\mu$ is increased further, coupled processes completely overcome $\tau_I$, even in the western basin (Fig. 11c), generating the spatial patterns characteristic of coupled feedbacks in absence of $\tau_I$.

To check the relative importance of the thermocline slope versus the upwelling induced by $\tau_{ext}$, we perform three experiments similar to those in the previous section, replacing the components of $\tau_{ext}$ by an equivalent upwelling. First, we replace $\tau_z$ by a constant upwelling $w_0 > 0$; the external wind stress is now only due to $\tau_I$. The external temperature field and the thermocline are presented in Fig. 12a, and although the thermocline is flat in the east, it is slightly shallower than the equilibrium value due to the easterlies in the west. At $\mu = 1.0$,

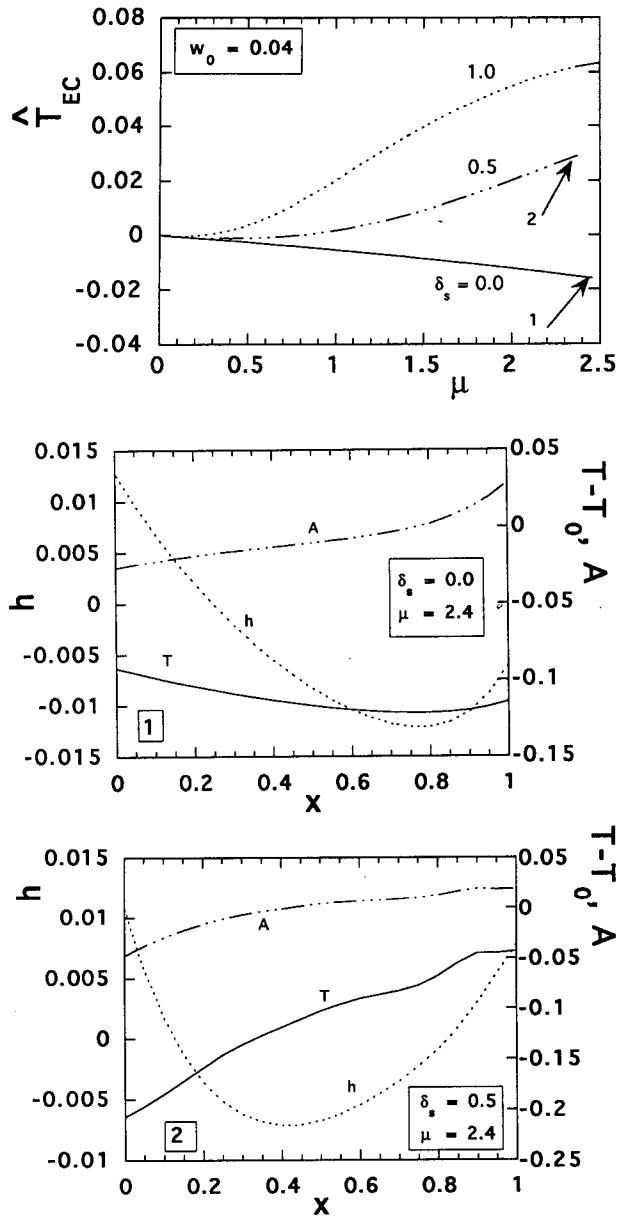


FIG. 10. Case of very small externally specified upwelling or entrainment velocity, $w_0 = 0.04$, in the modified model. (a) As in Fig. 2 but for several values of the surface-layer feedback: $\delta_s = 0$ (solid), $\delta_s = 0.5$ (dash–dotted), $\delta_s = 1.0$ (dashed). Other parameters standard. (b) As in Fig. 6b, but for labeled point 1 in (a), $\delta_s = 0$, $\mu = 2.4$. (c) As in (b) but point 2, $\delta_s = 0.5$, $\mu = 2.4$.

coupled processes have modified this situation into a climatology (Fig. 12b) similar to that in Fig. 11c. As in section 5, the externally forced thermocline slope is not important to the coupled processes determining the cold-tongue pattern.

Second, we replace $\tau_{ext}$ entirely by an equivalent spatially dependent upwelling given by

$$w_0(x) = -\delta_F[\tau_z + \tau_I(x)]\,. \qquad (6)$$

The upwelling is as before, but the thermocline is now flat over the whole basin. The externally forced SST field is shown in Fig. 13a, having a cold tongue right at the western coast. Coupling again modifies it to the cold-tongue pattern preferred by coupled processes, as shown in Fig. 13b.

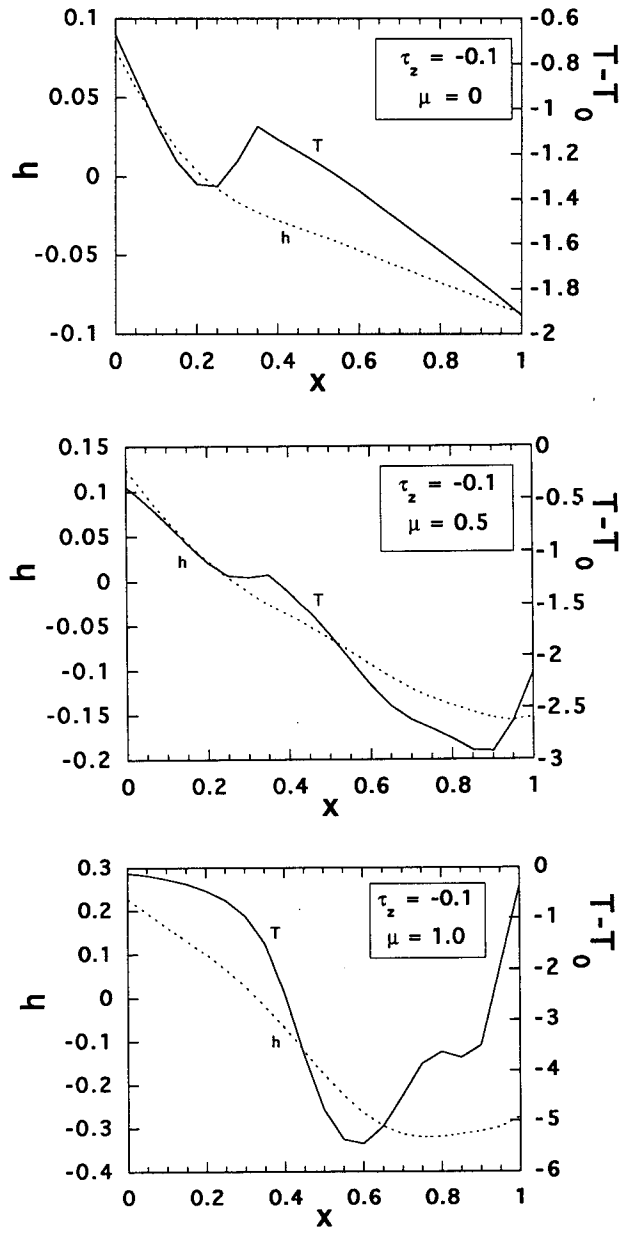


FIG. 11. As in Fig. 6b but for the case of spatially varying external wind stress, $\tau_{ext} = \tau_z + \tau_I$, with $\tau_I$ an increase in easterlies over the Indonesian region (see text), and $\tau_z = -0.1$ a zonally constant easterly component. (a) Uncoupled ocean solution forced by $\tau_{ext}$. (b) Standard coupling, $\mu = 0.5$. (c) $\mu = 1.0$. Other parameters standard.

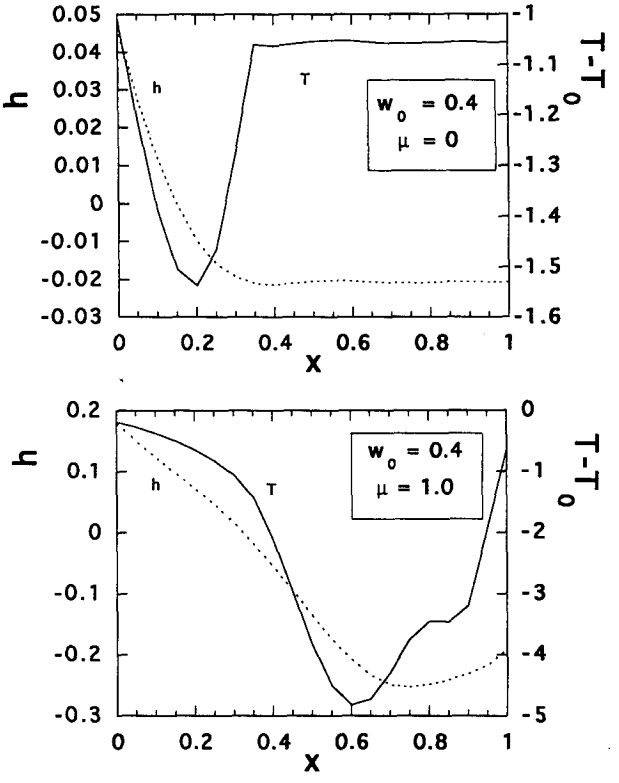


FIG. 12. As in Fig. 11, but for modified version of the model with $\tau_z$ replaced by specified entrainment velocity, $w_0 = 0.4$, but retaining $\tau_I$. (a) Uncoupled ocean solution, $\mu = 0$. (b) Coupled solution for $\mu = 1.0$.

Finally, we show that a sufficient magnitude of external upwelling or entrainment velocity (whether imposed by external windstress or created by sub-Reynolds-scale mixing) over a sufficient portion of the basin is important to get the right climatology. We take the limit $\tau_z \to 0$ and $w_0 \to 0$. The externally generated climatology (Fig. 14a) is now entirely due to $\tau_I$ and is similar to Fig. 12a, except that, because of the lack of upwelling in the east, the temperature is at the equilibrium value. When the coupling is turned on, westerlies are generated to the east of the cold tongue (Fig. 14b) that $\tau_I$ maintains in the west. These westerlies prevent the temperature in midbasin from becoming colder than $T_0$ since there is downwelling. However, easterlies are generated through spontaneous symmetry breaking in the eastern part of the basin. This is a process analogous to that found in Part I in a similar situation, where $\tau_I$ and $\tau_z$ were both zero and the cold tongue was created by a bifurcation from a $T = T_0$ state. At larger coupling, a complicated spatial structure (Fig. 14c) is created, similar to Fig. 7f of ND. This differs strongly from the spatial structures obtained with significant upwelling throughout the basin (e.g., Fig. 12b). Although the cold tongue in Fig. 14c is not realistic, the feedback processes do again succeed at modifying the $\tau_{ext}$ imposed structure at high coupling. When a very small amount of constant upwelling is added, this situation remains the same. The reason sufficiently strong external upwelling or entrainment must be present for the coupled processes to modify the cold tongue in a realistic manner is twofold. First and most important is that a reasonable strength of the thermocline feedback is required and thus there must be sufficient upwelling or entrainment to communicate subsurface temperature anomalies to the surface. When there is little external upwelling, the thermocline feedback tends to be small compared to the surface-layer feedback, which yields different characteristic patterns (e.g., Fig. 4b versus Fig. 4a). Second, if the cold tongue must generate itself spontaneously, much larger coupling is required than if there is an externally maintained cooling (relative to $T_0$) that can be magnified by the chain of coupled feedbacks.

## 7. Relevance for general circulation models

The results presented above seem generally consistent with the hypothesis that climate drift in tropical coupled GCMs can be due in part to the way three-

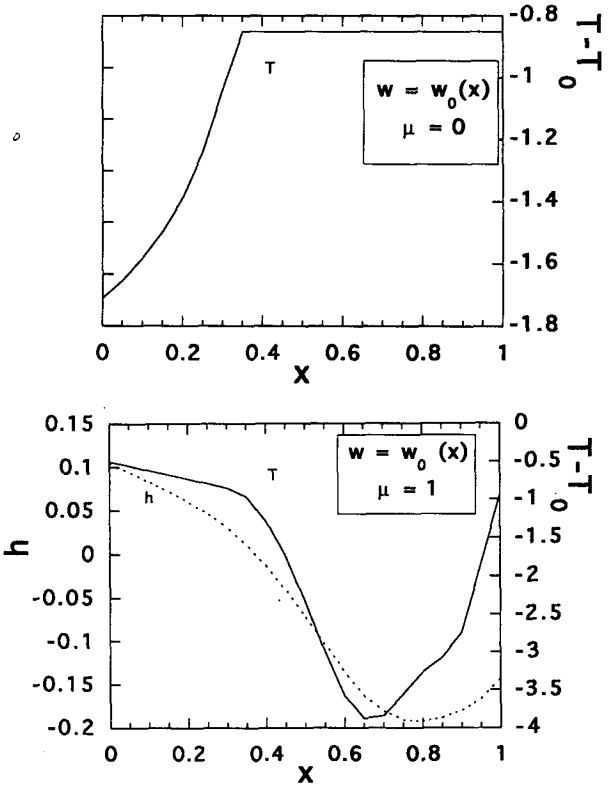


FIG. 13. As in Fig. 11 but replacing $\tau_{ext}$ by a specified upwelling of the same shape as that driven by $\tau_{ext}$ in the standard model. (a) Uncoupled ocean solution, $\mu = 0$. (b) Coupled solution for $\mu = 1.0$.

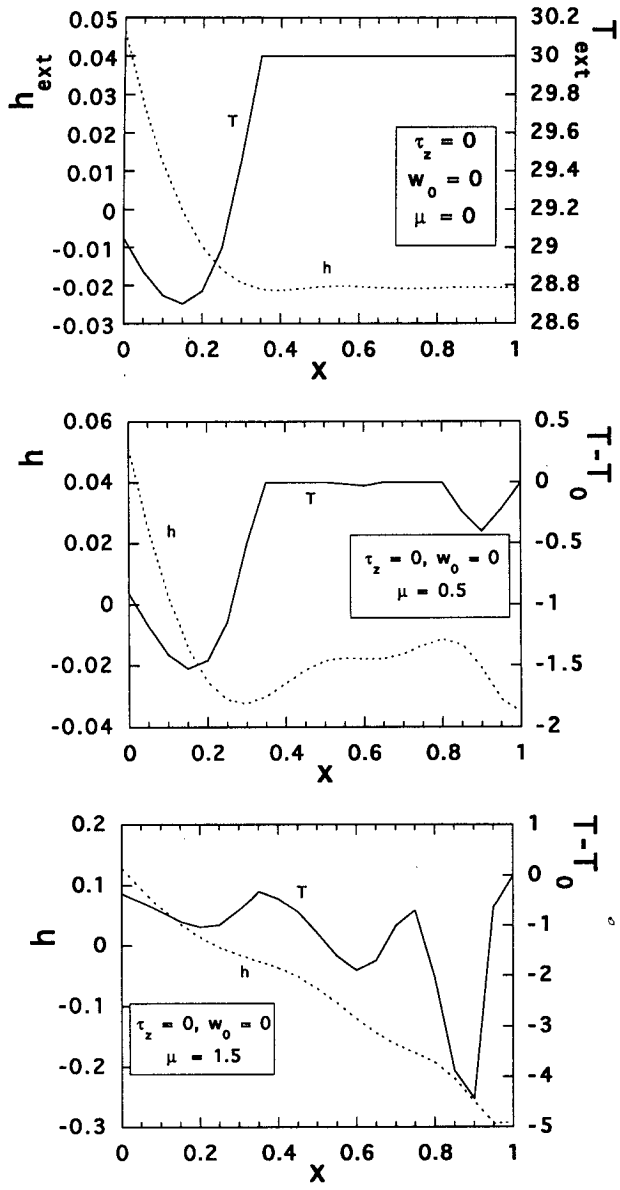


FIG. 14. As in Fig. 11 but with $\tau_z = 0$ and no entrainment velocity ($w_0 = 0$). (a) Uncoupled ocean solution, $\mu = 0$. (b) Coupled solution for $\mu = 0.5$. (c) Coupled solution for $\mu = 1.5$.

dimensional coupled feedbacks exacerbate an error in one component of the model. Here, we use model–model comparisons from the simple system, where we now have an understanding of the feedbacks, to provide specific examples of various ways coupled feedbacks affect climate drift. We emphasize that the number and complexity of physical mechanisms involved in coupled GCM feedbacks will be greater than those considered here. For instance, cloudiness feedbacks and the evaporation–wind feedback in the surface heat flux will be important, while here only wind stress feedbacks are active. Nonetheless, the simple model can be used to illustrate three basic scenarios that in essence will apply to more general physical feedback mechanisms. The specific wind stress feedbacks active here can thus provide suggestive prototypes for corresponding scenarios involving three-dimensional feedbacks in GCMs. In each scenario a control model equilibrium solution is taken to be the "true" solution, and the solution from a modified model is taken to contain the model error.

In scenario 1, the overall coupling strength is incorrect. Here the parameter $\mu$ controlling the magnitude of the wind stress feedbacks from the atmosphere is used. For example, we replot the standard parameter curve from Fig. 5 in Fig. 15a, considering two points along the curve to be the two model solutions: point 2 ($\mu = 1.0$) versus a control at point 1 ($\mu = 0.5$). Obviously, which run is taken as control can be reversed, and weak coupling is perhaps more likely as an error in current GCMs than strong coupling. The point of this scenario is merely that a simple error in the magnitude of the feedbacks, which in itself has no spatial variation, leads to an error field (Fig. 15b) that has

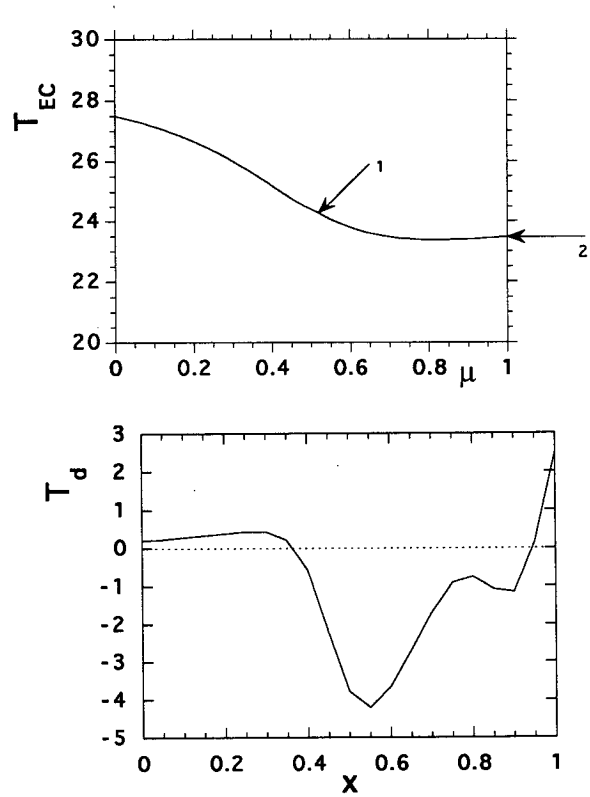


FIG. 15. Scenario 1 for climate drift: incorrect overall coupling strength. (a) As in Fig. 4 but showing total SST at the point $x = 0.7$ in the east-central Pacific as a function of coupling, for standard parameters ($\epsilon_a = 2.5$). Point 1 is considered the "correct" climatology, point 2 the example of drift due to strong coupling. (b) Climate drift SST error, $T_d$, for the difference between points 2 and 1 in (a).

spatial structure. This pattern is not merely due to a change in amplitude but involves changes in the shape of the cold tongue produced by nonlocal and nonlinear feedbacks. A modeler faced with diagnosing errors in this field might guess that the coupling was too strong but would be perplexed by the longitudinal structure. It is also easy to generate examples where the cold tongue shifts even more in position than the case shown.

In scenario 2, suppose that the uncoupled climatology has a small error. Even if this model error itself has no dependence on coupling, coupled feedbacks can act to exacerbate the error. For example, consider a slight error in processes that affect the surface heat-flux equilibrium temperature $T_0$, say, 1° lower ($T_0 = 29$) than the "correct" value. The bifurcation diagrams for both equilibrium temperatures are plotted in Fig. 16a (note that an intersection of the curves only implies that the error is zero at a particular index point in the east-central basin). Although the original error was evenly distributed in longitude, the spatial structure of the error field (Fig. 16b, shown for two values of coupling) has a signature that strongly depends on coupled dynamics. It can be magnified or reduced or even be of opposite sign than the original error. A modeler diagnosing the errors would correctly deduce the source of the problem in the western Pacific, where local processes happen to dominate, but might easily miss the mechanism that leads to warming in the east and the fact that the original cooling error applies in the east as well. The particular mechanism at work here is that the west is more susceptible to SST change by surface heat flux; since it tends to cool more, the SST gradient and hence the trades are reduced; the east thus tends to warm, thereby further reducing the trades.

In the last scenario, there is an error in a process that is directly involved in coupled feedbacks. We present the example of an error in vertical mixing processes that causes surface-layer upwelling to react too strongly to wind stress (large $\delta_s$). In this model, this is easily idealized to a situation where there is no error in the uncoupled system driven by $\tau_{ext}$, but as coupling is increased the solution branch deviates from the control. Bifurcation diagrams for standard $\delta_s$ and a slightly higher value ($\delta_s = 0.75$) are shown in Fig. 17a. The difference between the spatial structures for the high-$\delta_s$ case and the control are shown for $\mu = 0.5$ and $\mu = 1.0$ in Fig. 17b. As noted earlier, the preferred cold-tongue structure differs with stronger surface-layer feedbacks, including a shift of the cold tongue and warming near the eastern coast. The magnitude and shape of this error also depend on what strength of coupling applies. Again, a modeler faced with this error field would find it challenging to guess that a tendency to overly strong upwelling was responsible for both the cooling and warming in different parts of the basin. The area of warm water near the east coast in the strong

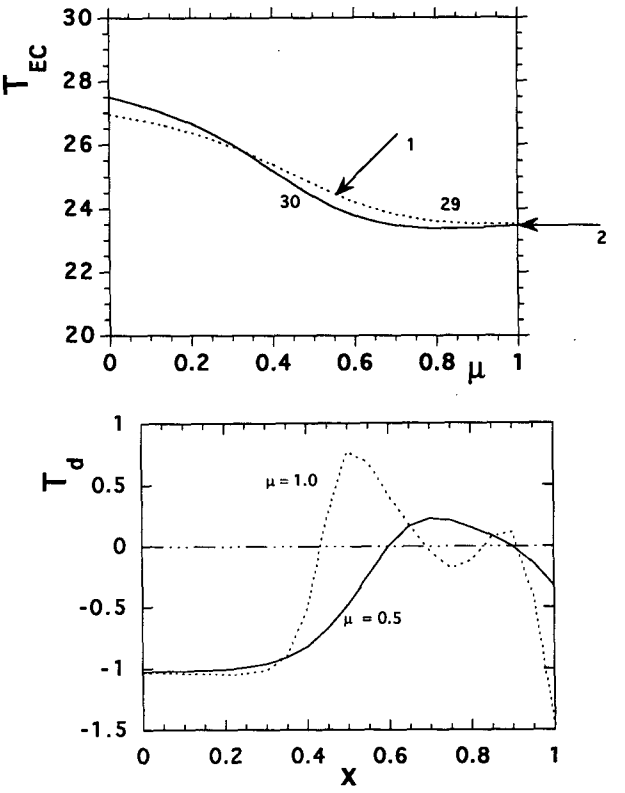


FIG. 16. Scenario 2 for climate drift: coupled processes feedback on an uncoupled error (error in a process independent of coupling). (a) As in Fig. 15a but for standard model (solid) versus drifted model (dashed) that has a 1°C error in $T_0$ (spatially constant). Labeled points indicate coupling values for which longitudinal plots of the error between the two models are shown in (b). (b) Climate drift SST error $T_d$ due to feedbacks on the $T_0$ error at two values of coupling, $\mu = 0.5$ and 1.0.

coupling case might be assumed to be due to inadequacies in coastal dynamics, whereas it is simply a consequence of the basin-wide solution. In fact, excessive coastal warming is common in coupled GCMs, and this might be a contributing mechanism.

In practice, sources of error will tend to combine elements from each of these scenarios. For instance, an error in an ocean mixing scheme or an error in representation of stratus clouds would actually affect both the externally driven solution (scenario 2) and the nature of the coupled feedbacks (scenario 3). The latter might be more important in the case of the mixing scheme, but in the stratus case both might be equally important. An error in a cumulus parameterization might affect the overall strength of coupling (scenario 1), as well as the relative importance of feedback mechanisms (scenario 3), even if it left the solution in absence of ocean dynamics relatively unchanged. The purpose of these scenarios is rather to build up intuition for the way nonlocal processes involving multiple-cou-

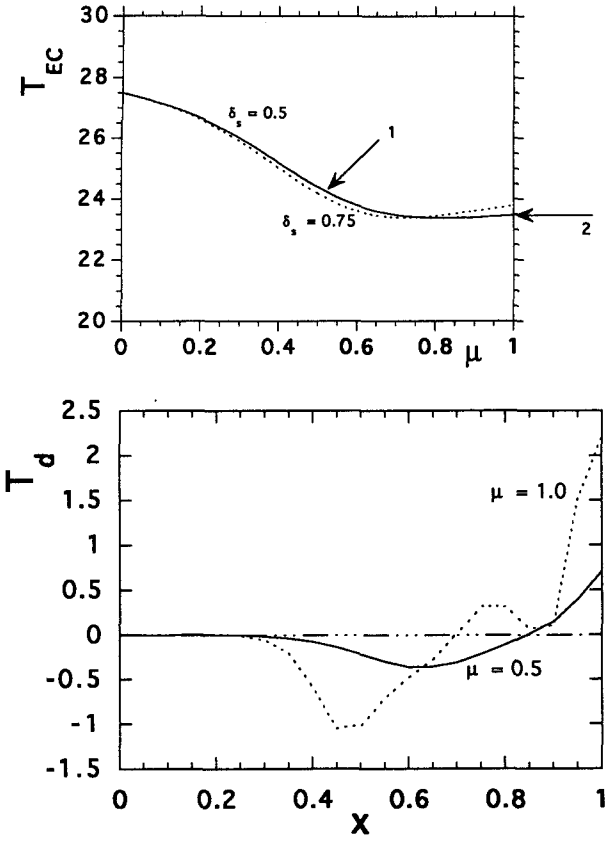


FIG. 17. Scenario 3 for climate drift: error in a process involved in coupled feedbacks. (a) As in Fig. 15a but for standard model (solid, $\delta_s = 0.5$) versus drifted model (dashed, $\delta_s = 0.75$) that has an error in the surface-layer parameter. Labeled points indicate coupling values for which longitudinal plots of the error between the two models are shown in (b). (b) Climate drift SST error $T_d$ due to the incorrect value of $\delta_s$ at two values of coupling, $\mu = 0.5$ and 1.0.

pled feedbacks turn relatively simple errors into complicated error fields.

If we accept that coupling feeds back on errors in representation of various processes and that the nonlocal nature of these feedbacks makes the source of error subtle to diagnose, why have coupled GCM simulations of the tropical climatology improved so impressively in the last few years [see intercomparisons by Neelin et al. (1992) and Mechoso et al. (1995)]? We suggest that because coupled feedbacks often inflated errors in the original model components far beyond what might have been expected from the uncoupled system, reducing errors in the model components has a correspondingly large effect in interrupting these error amplifications. Coupled GCM groups have, by and large, resisted the temptation to tune models region by region but have concentrated on improving known weak points. Such improvements tend to be exported throughout the coupled feedback loops.

## 8. Discussion

In a simple prototype system for coupled feedbacks between SST, Walker circulation, and ocean dynamics, we found in Part I that these interactions were important to the climatology of the equatorial Pacific ocean and trade winds. Here we show how these coupled feedbacks create a preferred shape for the cold-tongue–warm-pool configuration and on what mechanisms this shape depends.

Despite its simplifications, the model proves capable of simulating a reasonable facsimile of the cold-tongue structure along the equator. We distinguish between the component of the wind stress that is associated with coupled feedbacks within the basin (i.e., with SST gradients due to ocean dynamics) and the contribution to wind stress that is due to processes external to the basin $\tau_{ext}$. Comparing the SST, thermocline depth, etc., that is driven by $\tau_{ext}$ in the uncoupled ocean to the pattern obtained in the coupled model, it is found that as the strength of coupling increases, the spatial pattern evolves into a form considerably different than the uncoupled case. This structure is not extremely sensitive to small changes in model parameters. However, larger changes in certain parameters—notably those affecting the relative importance of the feedbacks involving thermocline changes and upwelling changes, respectively—cause substantial modification in the position and shape of the cold tongue. The thermocline feedback tends to move the cold tongue eastward and favors broad spatial extent. The upwelling feedback tends to move the cold tongue westward. Depending on other factors, the upwelling feedback can narrow the cold tongue in the central basin or can create longitudinal variations of shorter spatial scale within the cold tongue. In an extreme case, it is possible to develop a cold tongue that is strongest in the western basin. Thus, the balance of processes involved in the internal feedbacks is crucial to determining the shape of the cold tongue and the position of the warm-pool margin.

The external wind stress plays a role as well, but it differs from what might be anticipated from the uncoupled ocean problem. For example, a zonally constant wind stress of a magnitude suitable for the zonal-average Hadley circulation acting on the uncoupled ocean creates a weak cold tongue. The coldest water is found at the very east of the basin (without a broad minimum) due to the slope of the thermocline induced by the winds. In the coupled problem, the feedbacks produce a self-consistent solution with the trade winds in a broad maximum across the center of the basin associated with the broad minimum in SST in the east-central basin, and vice versa. The thermocline slope associated with $\tau_{ext}$ is of secondary importance to this process, since the feedbacks easily generate enough thermocline slope in the central basin without it. The

most important roles of the externally forced contribution to the cold tongue are as follows.

(i) To create a basic cooling on which the coupled processes can then feedback to amplify the cold tongue. The size of this externally maintained cooling strongly affects the magnitude of the cold tongue that can be attained at reasonable values of the coupling. However, it has little effect on the shape of the cold tongue.

(ii) To provide a basic upwelling along the equator so that thermocline variations are communicated to the surface to affect SST. If this externally forced contribution to the upwelling is small, coupled processes alone can still generate a cold tongue because increased trades tend to increase upwelling, which amplifies the cold tongue, etc. However, the shape of the resulting cold tongue differs from observed because the upwelling feedback dominates over the thermocline feedback.

These results lead to a more quantified version of some of the mechanisms involved in the climatological version of the Bjerknes hypothesis stated in Part I. Large-scale easterlies, especially those involved in the global Hadley circulation, create some cooling and upwelling in the equatorial Pacific. This externally maintained contribution acts as a forcing or seed for a chain of coupled feedbacks. At weak coupling this can be viewed as a linear amplification and modification of the externally maintained signal, but at higher coupling the nonlinear solution depends little on the details of the external contribution. The chain can be narrated as follows: the external stress creates cooling relative to a state without feedbacks; the SST gradients drive additional easterlies over much of the basin; these cause more upwelling and thermocline perturbation; the upwelling causes cooling under the easterlies, while the thermocline slope under the easterlies implies cooling toward the east; this cooling further increases the trades, especially to the west of the main cooling region; the net result of these interactions determines a cooling larger than the externally forced seed and with a preferred shape.

The processes setting the preferred shape can be complex, but we can draw on parallels to analytical results for the linear coupled mode problem considered in Jin and Neelin (1993b). The thermocline feedback favors large scales both in ocean and atmosphere but particularly in the ocean because of east–west communication by lightly damped oceanic equatorial wave dynamics. Both components have an east–west asymmetry in their response (due to $\beta$): the thermocline responds to easterlies by shallowing to the east and furthermore experiences a shallowing of its zonal average due to the net effects of basin adjustment by wave dynamics, such that deepening to the west is less. The atmospheric response to cooling has net easterlies, over and to the west of the anomaly, with lesser westerlies to the east. A self-consistent pattern can thus be set up with a broad cooling in the east-central basin, yielding easterlies across the basin, maximum in midbasin (the smaller westerlies to the east mostly lie over land); the thermocline response yields a minimum depth and hence cooling with a broad maximum in the east-central basin and the strongest SST gradient across midbasin. On the other hand, the upwelling feedback depends on the atmosphere to set spatial scales because upwelling is local under the wind stress. While the upwelling feedback can assist the thermocline feedback in amplifying the cold tongue, it tends to shift the pattern westward under the strongest westerlies.

A clear illustration of the role of coupled feedbacks, as opposed to external forcing, in determining the spatial pattern in this model is provided by the case where the external forcing is modified by adding easterlies in the western Pacific. Whereas this creates a western cold tongue in the uncoupled ocean, in the coupled model the feedbacks largely overcome this tendency and produce a cold tongue and warm pool similar to the standard case.

Thus the position and spatial pattern of the observed broad cold tongue in the central to eastern Pacific is primarily determined by the coupled feedback involving SST, wind, and thermocline depth, with external forcing playing a supporting role and upwelling feedbacks contributing secondary modifications.

While it is hard to devise simple tests of this hypothesis from observations, it can be tested in coupled GCMs. Some corroboration might be found in the serendipitous experiments carried out in coupled GCMs in the course of trying to correct climate drift. While the mechanisms of climate drift are more complex in GCMs than in the simple scenarios offered in section 7, we hope that these examples prove useful to the modeling community. Direct tests of the hypothesis may be carried out by comparing solutions from a coupled GCM that accurately simulates climatology to the uncoupled experiments prescribed in section 2 for diagnosing the externally forced part of the solution. The climatological version of the Bjerknes hypothesis predicts that the form, magnitude, and sensitivity of the coupled cold-tongue–warm-pool configuration will differ significantly from the uncoupled experiments.

One consequence of the hypothesis, if true, is that the impact of external climate variations upon the Pacific basin is best viewed in terms of interaction with a tightly coupled entity involving both ocean and atmosphere over the region, rather than in terms of effect upon one or the other in isolation. Another consequence is that the warm pool must be understood in the context of larger-scale three-dimensional interactions. The deep thermocline and low trade wind magnitudes in the Western Pacific allow local interactions and vertical processes within the warm pool and the atmosphere above it to be the principal factors determining SST. However, the winds and thermocline in

the warm pool region are both set by nonlocal coupled processes over the entire basin. The extent of the warm pool, that is, the boundary with the companion cold tongue, is thus determined by basin-scale processes. The prototype presented here for these basin-wide interactions may provide useful background for interpreting results from the TOGA-COARE and CEPEX field experiments, which by necessity were focused locally within subregions of the Pacific-coupled system.

*Acknowledgments.* This work was supported in part by National Science Foundation Grant ATM-9215090, National Oceanic and Atmospheric Administration Grant NA46GPO244 (JDN) and NOP-Project 853110 (HD). This work was initiated during a visit of HD to UCLA in November 1992, continued during a second visit in November 1993, and during a visit by JDN to M.I.T. Support for the first visit of HD was obtained through a travel grant from the Nederlandse Organisatie voor Wetenschappelijk Onderzoek (Netherlands Organization for Scientific Research, NWO) and for the second through National Science Foundation Grant ATM-9158294. JDN was supported at M.I.T. by the Henry G. Houghton Fund and the Department of Earth, Atmospheric and Planetary Sciences. All computations were performed on the CRAY Y-MP at the Academic Computer Centre (SARA), Amsterdam, the Netherlands. Use of these computing facilities was sponsored by the Stichting Nationale Supercomputer Faciliteiten (National Computing Facilities Foundation, NCF), with financial support from the Nederlandse Organisatie voor Wetenschappelijk Onderzoek (Netherlands Organization for Scientific Research, NWO). One of authors (HD) thanks Will de Ruijter (I.M.A.U.) for much encouragement and support. Discussions with Peter Stone and George Philander and with the participants in the coupled GCM intercomparison meetings organized by Pascale Delecluse and Roberto Mechoso are appreciated.

## APPENDIX

## Model

The atmospheric Gill model used for the operator $A$ in (1), evaluated for equatorial wind stress, is given by

$$A(T') = 2\exp(3\epsilon_a x)\int_x^1 \exp(-3\epsilon_a s)T'(s)ds - \frac{2}{3}\exp(-\epsilon_a x)\int_0^x \exp(\epsilon_a s)T'(s)ds\,, \quad \text{(A1)}$$

TABLE A1. Standard values of secondary parameters (nondimensional).

| | | |
|---|---|---|
| $\eta_1 = 6.667$ | $\eta_2 = 0.833$ | $\delta_F = 4.104$ |
| $T_N = T_0 = 30°C$ | $T_{so} = 24°C$ | $\epsilon_w = 0.694$ |

where $\epsilon_a$ is the dimensionless atmospheric damping, and $T' = T - T_0$ is the departure of SST from surface heat-flux equilibrium.

The equatorial-band SST equation is given by

$$\partial_t T = -\mathscr{H}(w_1)w_1(T - T_s) + \mathscr{H}(-v_N)v_N(T - T_N) - \epsilon_T(T - T_0)\,, \quad \text{(A2)}$$

where $\mathscr{H}$ is a continuous approximation to the Heaviside function, $w_1$ is the vertical velocity, $v_N$ is the off-equatorial meridional velocity, $\epsilon_T$ is the thermal damping, and $T_s$ is the subsurface temperature. The surface heat-flux equilibrium temperature $T_0$ is taken as spatially constant to highlight the spatial structure produced by purely dynamical feedbacks. The velocities $w_1$ and $v_N$, created by Ekman dynamics, are given by

$$v_N = w_1 = -\delta_F \tau_{\text{ext}}(x) - \mu\delta_s A(T - T_0) \quad \text{(A3)}$$

if we take the characteristic depth of upwelling equal to the mixed-layer depth. The subsurface temperature $T_s$ depends on the equatorial thermocline depth $h$ according to

$$T_s(h) = T_{so} + (T_0 - T_{so})\tanh(\eta_1 h + \eta_2)\,, \quad \text{(A4)}$$

with $\eta_1 = H/H_*$, $\eta_2 = h_0/H_*$, where $h_0$ and $H_*$ control the steepness and the offset of the $T_s$ profile. The parameter $T_{so}$ is quantitatively important for a given $\mu$, but it is trivial in the sense that given a solution as a function of $\mu$ for one value of $T_{so}$, the (nonlinear) solution for another value of $T_{so}$ can be obtained by rescaling $(T_0 - T)$ and $\mu$. Thus $T_{so}$ affects the magnitude of the cold tongue but not the essential physics. Standard values of parameters are given in Table A1.

For the ocean model the steady thermocline response at the equator is given by

$$h(x) = \int_0^1 s^{1/2}\tau(s)ds - \int_x^1 \tau(s)ds\,. \quad \text{(A5)}$$

The constant of integration in (A5) contains information about the net result of adjustment in a finite basin by two-dimensional wave dynamics in an approximation where latitudinal variation of windstress is slow and ocean damping time is much larger than the Kelvin wave crossing time (Neelin and Jin 1993). Off-equatorial thermocline depth perturbations can be evaluated diagnostically if desired.

## REFERENCES

Bjerknes, J., 1969: Atmospheric teleconnections from the equatorial Pacific. *Mon. Wea. Rev.*, **97**, 163–172.

Chervin, R. M., and L. M. Druyan, 1984: The influence of ocean surface temperature gradient and continentality on the Walker circulation. Part I: Prescribed tropical changes. *Mon. Wea. Rev.*, **112**, 1510–1523.

Dijkstra, H. A., and J. D. Neelin, 1995: On the attractors of an intermediate coupled equatorial ocean–atmosphere model. *Dyn. Atmos. Oceans*, in press.

Endoh, M., T. Tokioka, and T. Nagai, 1991: Tropical Pacific sea surface temperature variations in a coupled atmosphere–ocean general circulation model. *J. Mar. Systems,* **1,** 293–298.

Gent, P. R., and J. J. Tribbia, 1993: Simulation and predictability in a coupled TOGA model. *J. Climate,* **6,** 1843–1858.

Hao, Z., J. D. Neelin, and F. F. Jin, 1993: Nonlinear tropical air-sea interaction in the fast wave limit. *J. Climate,* **6,** 1523–1544.

Jin, F. F., and J. D. Neelin, 1993a: Modes of interannual tropical ocean–atmosphere interaction—a unified view. Part I: Numerical results. *J. Atmos. Sci.,* **50,** 3477–3503.

——, and ——, 1993b: Modes of interannual tropical ocean–atmosphere interaction—a unified view. Part III: Analytical results in fully coupled cases. *J. Atmos. Sci.,* **50,** 3523–3540.

Latif, M., A. Sterl, E. Maier-Reimer, and M. M. Junge, 1993: Climate variability in a coupled GCM. Part I: The tropical Pacific. *J. Climate,* **6,** 5–21.

——, T. Stockdale, J. Wolff, G. Burgers, E. Maier-Reimer, M. M. Junge, K. Arpe, and L. Bengtsson, 1994: Climatology and variability in the ECHO coupled GCM. *Tellus,* **46A,** 351–366.

Lau, N. C., S. G. H. Philander, and M. J. Nath, 1992: Simulation of El Niño–Southern Oscillation phenomena with a low-resolution coupled general circulation model of the global ocean and atmosphere. *J. Climate,* **5,** 284–307.

Mechoso, C. R., C.-C. Ma, J. D. Farrara, J. Spahr, and R. W. Moore, 1993: Parallelization and distribution of a coupled atmosphere–ocean general circulation model. *Mon. Wea. Rev.,* **121,** 2062–2076.

——, A. W. Robertson, N. Barth, M. K. Davey, P. Delecluse, P. Gent, B. Kirtman, M. Latif, T. Nagai, S. G. H. Philander, P. S. Schopf, T. Stockdale, M. J. Suarez, O. Thual, and J. Tribbia, 1995: The seasonal cycle over the tropical Pacific in general circulation models. *Mon. Wea. Rev.,* in press.

Meehl, G. A., 1990: Development of global coupled ocean–atmosphere general circulation models. *Climate Dyn.,* **5,** 19–33.

Mitchell, T. P., and J. M. Wallace, 1992: The annual cycle in equatorial convection and sea surface temperature. *J. Climate,* **5,** 1140–1156.

Nagai, T., T. Tokioka, M. Endoh, and Y. Kitamura, 1992: El Niño Southern Oscillation simulated in an MRI atmosphere–ocean coupled general circulation model. *J. Climate,* **5,** 1202–1233.

Neelin, J. D., 1991: The slow sea surface temperature mode and the fast-wave limit: Analytic theory for tropical interannual oscillations and experiments in a hybrid coupled model. *J. Atmos. Sci.,* **48,** 584–606.

——, and M. Latif, 1992: Tropical air-sea interaction in general circulation models. *Climate Dyn.,* **7,** 73–104.

——, and F. F. Jin, 1993: Modes of interannual tropical ocean–atmosphere interaction—a unified view. Part II: Analytical results in the weak-coupling limit. *J. Atmos. Sci.,* **50,** 3504–3522.

——, and H. A. Dijkstra, 1995: Ocean–atmosphere interaction and the tropical climatology. Part I: The dangers of flux-correction. *J. Climate,* in press.

Philander, S. G. H., R. C. Pacanowski, N. C. Lau, and M. J. Nath, 1992: Simulation of ENSO with a global atmospheric GCM coupled to a high-resolution, tropical Pacific ocean GCM. *J. Climate,* **5,** 308–329.

Robertson, A. W., C.-C. Ma, C. R. Mechoso, and M. Ghil, 1995: Simulation of the tropical Pacific climate with a coupled ocean–atmospheric general circulation model. Part I: The seasonal cycle. *J. Climate,* in press.

Sperber, K. R., S. Hameed, W. L. Gates, and G. L. Potter, 1987: Southern Oscillation simulated in a global climate model. *Nature,* **329,** 140–142.

Stone, P. H., and R. M. Chervin, 1984: The influence of ocean surface temperature gradient and continentality on the Walker circulation. Part II: Prescribed global changes. *Mon. Wea. Rev.,* **112,** 1524–1534.

Xie, S.-P., 1994: The maintenance of an equatorially asymmetric state in a hybrid coupled GCM. *J. Atmos. Sci.,* **51,** 2602–2612.

——, and S. G. H. Philander, 1994: A coupled ocean–atmosphere model of relevance to the ITCZ in the eastern Pacific. *Tellus,* **46A,** 340–350.

Yamagata, T., and Y. Masumoto, 1989: A simple ocean–atmosphere coupled model for the origin of warm El Niño Southern Oscillation event. *Phil. Trans. Roy. Soc. London, A,* **329,** 225–236.